JOURNAL OF GUIDANCE, CONTROL, AND DYNAMICS
Vol. 24, No. 5, September–October 2001

Linear-Parameter-Varying/Loop-Shaping H_∞ Synthesis for a Missile Autopilot

A. Hiret* and G. Duc†
École Supérieure d'Electricité, F91192 Gif-sur-Yvette, France
J. P. Friang‡
Aerospatiale, F92320 Châtillon, France
and
D. Farret§
École Supérieure d'Electricité, F91192 Gif-sur-Yvette, France

The design of a gain-scheduled autopilot for a bank-to-turn missile over a wide operating range is considered. The main steps to obtain such a controller are explained. From a modeling point of view, the required linear fractional transformation of the gain-scheduled model is obtained by using polynomial expressions for each varying coefficient and a multivariable reduction procedure. Then a multivariable linear parametrically varying synthesis is performed in the spirit of the H_∞ /loop-shaping approach: the performance of the closed-loop system is defined by the use of compensators that depend on the altitude; this framework allows for adaptation to enhance the performance of the system because the specifications change considerably over the flight envelope. The gain-scheduled controller is then obtained by solving linear matrix inequalities and then reducing using again the multivariable reduction procedure. Lots of time- and frequency-domain analyses allow one to check the specifications: robust stability and performance analyses are proceeded by use of the structured singular value; nonlinear simulations using a six-degree-of-freedom model are also performed.

Nomenclature

a_y	=	lateral acceleration
a_z	=	normal acceleration
Cl_p	=	roll-moment coefficient
$Cl_{\alpha\beta}$	=	Dutch roll coefficient
Cl_ξ	=	roll-moment efficiency
$C_{m\alpha}, C_{m\eta}, C_{mq}$	=	normal moment coefficients
$C_{n\beta}, C_{n\zeta}, C_{nr}$	=	lateral moment coefficients
$C_{y\beta}, C_{y\zeta}, C_{yr}$	=	lateral force coefficients
$C_{z\alpha}, C_{z\eta}, C_{zq}$	=	normal force coefficients
$F_l(\boldsymbol{P}, K)$	=	lower LFT: $\boldsymbol{P}_{11} + \boldsymbol{P}_{12}K(I - \boldsymbol{P}_{22}K)^{-1}\boldsymbol{P}_{21}$
$F_u(\boldsymbol{G}, \Delta)$	=	upper LFT: $\boldsymbol{G}_{22} + \boldsymbol{G}_{21}\Delta(I - \boldsymbol{G}_{11}\Delta)^{-1}\boldsymbol{G}_{12}$
I_n	=	identity $n \times n$ matrix
J_x, J_y, J_z	=	moments of inertia
L	=	reference length
M	=	Mach number
m	=	missile mass
p	=	roll rate
Q	=	dynamic pressure
q	=	pitch rate
r	=	yaw rate
V	=	missile velocity
z	=	altitude
α	=	angle of attack
β	=	slideslip angle
ζ_{co}	=	commanded rudder deflection
ζ_{ex}	=	executed rudder deflection
η_{co}	=	commanded elevator deflection
η_{ex}	=	executed elevator deflection
ξ_{co}	=	commanded aileron deflection
ξ_{ex}	=	executed aileron deflection
τ	=	66% specified rise time
φ	=	bank angle
$0_{n\times m}$	=	null $n \times m$ matrix

Received 13 July 1999; revision received 4 August 2000; accepted for publication 12 January 2001.

*Graduate Student, Service Automatique, 3 rue Joliot-Curie; currently EDF/DRD, 6 quai Watier, F78401 Chatou, France; Arnaud.Hiret@edf.fr.
†Professor, Service Automatique, 3 rue Joliot-Curie; Gilles.Duc@supelec.fr.
‡Research Engineer, 2 rue Béranger.
§Ph.D. Student, Service Automatique, 3 rue Joliot-Curie; Damien.Farret@missiles.aeromatra.com.

I. Introduction

MODERN aircraft and missiles present an interesting challenge to autopilot design because the dynamics are highly time varying and cross coupled. To control such plants over a large operating domain, the controller has to be scheduled using exogenous variables (such as velocity, altitude, etc.) or internal ones (angle of attack, etc.).

To obtain scheduled autopilots, the engineers usually design controllers at distinct operating conditions and interpolate them. For example, scheduled missile autopilots have been designed using the linear quadratic Gaussian approach in Ref. 1 and using the H_∞ theory in Refs. 2 and 3; switched controllers designed using μ synthesis have also been developed in Ref. 4.

In recent years the emergence of new methods based on linear matrix inequalities (LMI) has offered new perspectives to obtain self-scheduled autopilots in a more systematic way (Refs. 5 and 6). As an advantage, the scheduled controller is obtained in a single step by considering the whole domain of operating conditions without requiring repeated designs. On the other hand, more attention must be given to obtain a linear parameter-varying (LPV) model of the plant.

For linear time-invariant plants it is well known that robust controllers with a high level of performance can be designed using H_∞ methods and particularly using the H_∞/loop-shaping approach.[7] The objective of this paper is to demonstrate that an efficient LPV controller can be designed for a six-degree-of-freedom (DOF) bank-to-turn (BTT) missile controlled by a tail deflection by considering the following steps:

1) The model of the missile is written as an LPV system whose varying parameters are the Mach number and the altitude and put on a linear fractional transformation (LFT) form.

2) A new parametric reduction procedure, based on the generalized gramians,[8] is defined to reduce the size of the LFT.

3) The plant model is shaped according to the H_∞/loop-shaping approach, where LPV compensators allow for adaptation to enhance

the specified performance and robustness according to the evolution of the parameters.

4) An LPV controller is designed for the shaped plant by solving LMIs,[9] which is further reduced using the same parametric reduction procedure.

This approach is of practical and theoretical interest. First it allows the extension to a large operating domain of the good behavior previously obtained on a fixed flight point using the H_∞/loop-shaping approach.[10] On the other hand, global stability and performance are guaranteed for the synthesis LPV model, for all values of the scheduling parameters and irrespective of their rate of variation.[9] Whenever the identification procedure yields a sufficiently accurate model, one can expect that such properties are also obtained for the actual plant.

The paper is organized as follows. Section II describes the LPV missile model and the design objectives. In Sec. III an LFT representation of the LPV model is first obtained, and a multidimensional parametric reduction procedure is developed. Section IV contains a brief summary of the H_∞/loop-shaping design and the LPV method and describes the design of the parametric multivariable autopilot. Section V is devoted to time- and frequency-domain linear analyses in order to check the specifications on the whole flight envelope. Besides it contains robust stability and performance analyses. Finally nonlinear six-DOF simulations reflecting actual flight conditions are presented in Sec. VI.

II. Missile Model and Control Problem

A. Aerodynamic Model and Control Scheme

Small-angle approximation of the dynamic model of a missile leads to the following equations:

$$\dot{\alpha} \approx \frac{QS}{mV}\left(C_{z\alpha}\alpha + C_{z\eta}\eta_{\text{ex}} + \frac{L}{V}C_{zq}q\right) + q - p\beta$$

$$\dot{q} \approx \frac{QSL}{I_y}\left(C_{m\alpha}\alpha + C_{m\eta}\eta_{\text{ex}} + \frac{L}{V}C_{mq}q\right) - \frac{J_z - J_x}{J_y}pr$$

$$\dot{\beta} \approx \frac{QS}{mV}\left(C_{y\beta}\beta + C_{y\zeta}\zeta_{\text{ex}} + \frac{L}{V}C_{yr}r\right) - r + p\alpha$$

$$\dot{r} \approx \frac{QSL}{I_z}\left(C_{n\beta}\beta + C_{n\zeta}\zeta_{\text{ex}} + \frac{L}{V}C_{nr}r\right) + \frac{J_x - J_y}{J_z}pq$$

$$\dot{p} \approx \frac{QSL}{I_x}\left(Cl_{\alpha\beta} + Cl_{\xi}\xi_{\text{ex}} + \frac{L}{V}Cl_{p}p\right) + \frac{J_y - J_z}{J_x}qr$$

$$\dot{\varphi} \approx p, \qquad a_z \approx V(\dot{\alpha} - q + p\beta), \qquad a_y \approx V(\dot{\beta} + r - p\alpha) \quad (1)$$

From a control synthesis point of view, the plant measurements are a_z, a_y, φ, q, r, and p (Fig. 1). The control inputs are η_{ex}, ζ_{ex}, and ξ_{ex}. The model (1) has to be augmented by one actuator and one delay on each channel; they are assumed to be described, respectively, by a second-order model and a first-order Padé approximation.

Because a BTT missile is considered, the objective of the autopilot is to control normal acceleration a_z and bank angle φ (pitch and roll channels) while maintaining the lateral acceleration a_y to zero (yaw channel).

In such a problem, the coupling terms between the pitch axis (on one hand) and the yaw and roll axes (on the other hand) are almost negligible. It is therefore more convenient to design separately an autopilot for the pitch axis and one for the yaw/roll axes by assuming perfect decoupling. The nonlinear simulations will allow us to check the relevance of this approach.

The flight envelope to be considered in this problem is shown in Fig. 2. The trajectory of the missile is predefined and must follow the nominal trajectory characterized by the bold line. The autopilot has also to guarantee a good behavior for perturbed trajectories, which are shifted by Mach 0.1 from the nominal one.

Over this wide field a gain-scheduled autopilot has to be designed. The aerodynamic forces and moments depend on M, z, α, and β. However, unlike what is done in Ref. 5, the range of variations of the angle of attack α is quite small on almost the whole flight envelope. It presumes that an α-independent autopilot can guarantee a good performance. Besides, α is not directly measured on line. Furthermore the variations of β remain small for a BTT missile. For these reasons neither α nor β will be taken as scheduling parameters. Once again, the nonlinear simulations will allow us to justify these choices and to verify the robustness with respect to the variations of α supported by the missile.

B. Design Objectives

The controller has to ensure the following specifications for all possible flight conditions: 1) 66% rise times lower than specified values for the pitch and roll channels: the value for $z = 0$, which is denoted τ, is gradually relaxed until 4τ for $z = z_{\max}$; 2) limitations on the first and second derivatives of η_{ex}, ζ_{ex}, and ξ_{ex}; 3) gain, phase, and delay margins: at least 7 dB, 40 deg, and 0.1τ for the inner, outer, and equivalent loops (points 3, 2, and 1 on Fig. 1, respectively) for the single-input pitch channel and at least 6 dB, 30 deg, and 0.1τ for the multi-input yaw-roll channel; and 4) for all maneuvers reasonably damped closed-loop responses and reasonably measurement noise reduction for high frequency.

Obviously, the specifications are normalized by τ for confidentiality reasons. However the chosen value for τ is the exact value of the rise time required at $z = 0$ for any pilot synthesized for this missile, which in addition is satisfied by a pilot developed earlier using classical frequency-domain methods. The reader

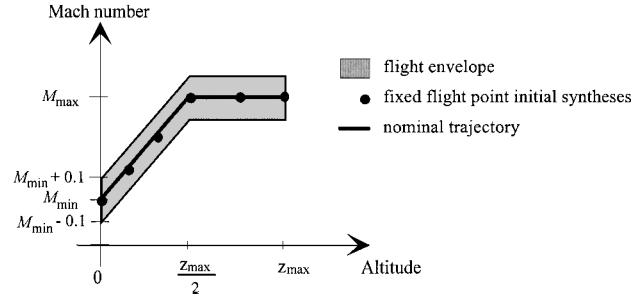

Fig. 2 Flight envelope.

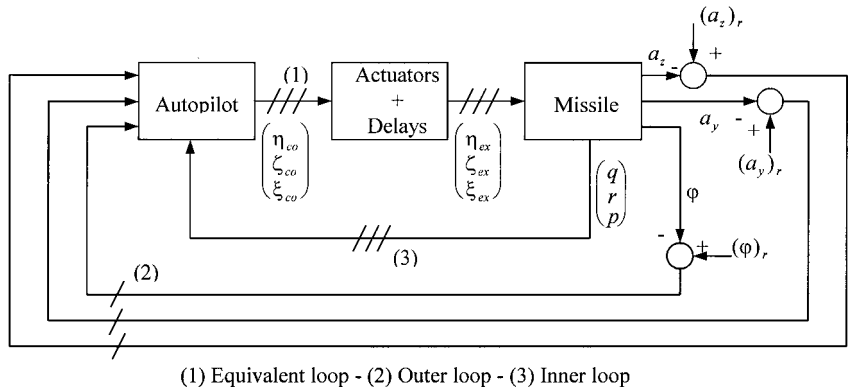

(1) Equivalent loop - (2) Outer loop - (3) Inner loop

Fig. 1 Control structure.

will therefore be able to evaluate the performance of the proposed design.

III. LFT Form of the Missile Model

A. LFT Missile Model

To obtain a gain-scheduled controller, the framework, which is further used, requires an LPV model written as a LFT.[11] Local linearization of Eqs. (1) leads to the following state-space representation, with $x = (a_z \;\; q \;\; a_y \;\; r \;\; \varphi \;\; p \;\; \eta_{ex} \;\; \dot{\eta}_{ex} \;\; \zeta_{ex} \;\; \dot{\zeta}_{ex} \;\; \xi_{ex} \;\; \dot{\xi}_{ex})^T$, $y = (a_z \;\; q \;\; a_y \;\; r \;\; \varphi \;\; p)^T$, and $u = (\eta_{co} \;\; \zeta_{co} \;\; \xi_{co})^T$:

$$\dot{x} = \begin{pmatrix} a_1 & a_2 & 0 & 0 & 0 & 0 & a_3 & a_4 & 0 & 0 & 0 & 0 \\ a_5 & a_6 & 0 & 0 & 0 & 0 & a_7 & 0 & 0 & 0 & 0 & 0 \\ 0 & 0 & a_8 & a_9 & a_{10} & a_{11} & 0 & 0 & a_{12} & a_{13} & 0 & 0 \\ 0 & 0 & a_{14} & a_{15} & 0 & 0 & 0 & 0 & a_{16} & 0 & 0 & 0 \\ 0 & 0 & 0 & a_{17} & 0 & 1 & 0 & 0 & 0 & 0 & 0 & 0 \\ 0 & 0 & a_{18} & a_{19} & 0 & a_{20} & 0 & 0 & a_{21} & 0 & a_{22} & 0 \\ 0 & 0 & 0 & 0 & 0 & 0 & 0 & 1 & 0 & 0 & 0 & 0 \\ 0 & 0 & 0 & 0 & 0 & 0 & -\omega_0^2 & -2\xi\omega_0 & 0 & 0 & 0 & 0 \\ 0 & 0 & 0 & 0 & 0 & 0 & 0 & 0 & 0 & 1 & 0 & 0 \\ 0 & 0 & 0 & 0 & 0 & 0 & 0 & 0 & -\omega_0^2 & -2\xi\omega_0 & 0 & 0 \\ 0 & 0 & 0 & 0 & 0 & 0 & 0 & 0 & 0 & 0 & 0 & 1 \\ 0 & 0 & 0 & 0 & 0 & 0 & 0 & 0 & 0 & 0 & -\omega_0^2 & -2\xi\omega_0 \end{pmatrix} x + \begin{pmatrix} 0 & 0 & 0 \\ 0 & 0 & 0 \\ 0 & 0 & 0 \\ 0 & 0 & 0 \\ 0 & 0 & 0 \\ 0 & 0 & 0 \\ 0 & 0 & 0 \\ -\omega_0^2 & 0 & 0 \\ 0 & 0 & 0 \\ 0 & -\omega_0^2 & 0 \\ 0 & 0 & 0 \\ 0 & 0 & -\omega_0^2 \end{pmatrix} u$$

$$y = (I_6 \quad 0_{6\times 6})x \tag{2}$$

ω_0 and ξ are the natural frequency and the damping and the actuators. The 22 coefficients $(a_1, \ldots, a_{22})$ are functions of two exogenous parameters: the Mach number M and the altitude z.

To obtain algebraic expressions, a least-squares procedure is proceeded for all varying coefficients. It leads to 22 polynomials dependent on M and z, shaped as follows:

$$a_i(M, z) = a_{i0} + a_{i1}M + a_{i2}z + a_{i3}Mz + a_{i4}M^2 + a_{i5}z^2 + a_{i6}M^2z + a_{i7}Mz^2 + a_{i8}M^3 + a_{i9}z^3 \tag{3}$$

The obtained LPV missile model is then

$$\dot{x}(t) = A[M(t), z(t)]x(t) + Bu(t), \qquad y(t) = Cx(t) \tag{4}$$

From this algebraic expression an LFT representation of the state-space equations is obtained by using an LFT form for each parameter and collecting them. The resulting LFT is shaped as shown in Fig. 3, where the sizes of the blocks depending on M and z are $n_M = n_z = 220$: obviously, this modeling leads to large-scale matrices.

Exact reduction of this LFT is first considered using the approach proposed in Ref. 12: after normalization of the parameters, classical state-space minimality concepts can be applied by considering that reducing the size of one parameter block is the same problem as reducing a nonminimal discrete-time state-space representation.

Removing first the zI block and considering M as the "pseudo delay operator," an exact reduction is proceeded by removing the "uncontrollable" and/or "unobservable" pseudostates of the corresponding state-space realization. One proceeds then similarly by interchanging the roles of M and z.

Although the procedure is not guaranteed to yield to an LFT of minimal size, it allows one to obtain an LFT with smaller dimensions of the parameter dependent blocks, namely $n_M = 18$ and $n_z = 28$.

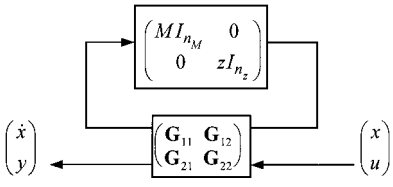

Fig. 3 LFT of the LPV missile model.

Because the complexity of the resulting controller depends on the model of the system, it is important to have an LFT as small as possible by keeping in mind the classical tradeoff between complexity and precision of the model. Additional reduction procedures have then to be defined and used.

B. Multidimensional Reduction Procedure

In Ref. 13 the notion of gramians have been extended to the case of LFTs with several time-varying parameters as in the LPV missile model. It allows us to define a reduction procedure based on balanced truncation, as in the linear classical case. Let us recall the main points of this theory.

The symmetric real matrices X and Y are generalized gramians of the LFT

$$F_u\left(\begin{bmatrix} \boldsymbol{G}_{11} & \boldsymbol{G}_{12} \\ \boldsymbol{G}_{21} & \boldsymbol{G}_{22} \end{bmatrix}, \Delta\right)$$

if

$$X \geq 0, \qquad Y \geq 0, \qquad \forall \Delta \in \underline{\Delta}, \qquad \Delta X = X\Delta, \qquad \Delta Y = Y\Delta$$

$$\boldsymbol{G}_{11}^T X \boldsymbol{G}_{11} - X + \boldsymbol{G}_{21}^T \boldsymbol{G}_{21} \leq 0, \qquad \boldsymbol{G}_{11} Y \boldsymbol{G}_{11}^T - Y + \boldsymbol{G}_{12}\boldsymbol{G}_{12}^T \leq 0 \tag{5}$$

where $\underline{\Delta}$ is the set of all admissible matrices Δ. The formulas (5) show that the gramians are solutions of two LMIs with a constraint on their structure.

If there exist singular generalized gramians, the Δ block of the LFT may be reduced with no error[14]: if $F_u(\boldsymbol{G}, \underline{\Delta})$ is well posed, balanced LFT representations exist so that $\tilde{X} = \tilde{Y} = \Sigma = \mathrm{diag}(\Sigma_i)$ with $\Sigma_i \in R^{n_i \times n_i}$ diagonal and $\Sigma_i \geq 0$. To obtain such realizations, we proceed as in the classical case by defining a transformation from the matrix T such as $XY = T\Sigma^2 T^{-1}$. Then $\tilde{Y} = TYT^T$ and $\tilde{X} = (T^{-1})^T X T^{-1}$ are generalized gramians of $F_u(\hat{\boldsymbol{G}}, \Delta)$, where

$$\hat{\boldsymbol{G}} = \begin{bmatrix} T^{-1}\boldsymbol{G}_{11}T & T^{-1}\boldsymbol{G}_{12} \\ \boldsymbol{G}_{21}T & \boldsymbol{G}_{22} \end{bmatrix} \tag{6}$$

As in the linear classical case, exact reduction is then proceeded by truncating in $\hat{\boldsymbol{G}}$ and Δ the rows and columns that correspond to the null eigenvalues of the product XY.

To obtain exact reduction, one should then seek for generalized gramians such that rank(XY) is minimum. This problem cannot be solved using directly the LMI techniques because of the nonconvex constraint on the rank. It is well known that such problems, which also arise for instance in designing reduced-order controllers,[15] are difficult to solve.

Considering further the nonnull eigenvalues of XY, an approximate reduction can be obtained. Suppose $F_u(\boldsymbol{G}_r, \Delta_r)$ is the reduced

model of $F_u(\hat{\boldsymbol{G}}, \Delta)$, then the structured induced 2-norm (see Ref. 8 for details about SI2-norm) of the reduction error is bounded by

$$\|F_u(\hat{\boldsymbol{G}}, \Delta) - F_u(\boldsymbol{G}_r, \Delta_r)\|_{SI2} \leq 2 \sum_i \sigma_i \tag{7}$$

where σ_i are the square roots of the truncated eigenvalues of XY (Ref. 8). Besides $F_u(\boldsymbol{G}_r, \Delta_r)$ is well posed. Based on this property, different algorithms have been developed in order to obtain generalized gramians X and Y with eigenvalues as small as possible. Their efficiency on the LFT modeling of the missile has been studied in Ref. 16. The most efficient one is to consider the following optimization problem.

$\max_{X^{-1}, Y^{-1}}$ trace $(X^{-1}Y^{-1})$ subject to:

$$X^{-1} \geq 0, \qquad Y^{-1} \geq 0$$

$$\forall \Delta \in \underline{\Delta}, \qquad \Delta X^{-1} = X^{-1}\Delta, \qquad \Delta Y^{-1} = Y^{-1}\Delta$$

$$\begin{bmatrix} -X^{-1} & X^{-1}\boldsymbol{G}_{11} & X^{-1}\boldsymbol{G}_{12} \\ \boldsymbol{G}_{11}^T X^{-1} & -X^{-1} & 0 \\ \boldsymbol{G}_{12}^T X^{-1} & 0 & -I \end{bmatrix} \leq 0$$

$$\begin{bmatrix} -Y^{-1} & Y^{-1}\boldsymbol{G}_{11}^T & Y^{-1}\boldsymbol{G}_{21} \\ \boldsymbol{G}_{11} Y^{-1} & -Y^{-1} & 0 \\ \boldsymbol{G}_{21} Y^{-1} & 0 & -I \end{bmatrix} \leq 0 \tag{8}$$

where Eqs. (8) are obtained from Eqs. (5) by using the Schur lemma.

This procedure still cannot be solved using LMI techniques because of the bilinear expression in the trace function. To obtain an LMI problem, an algorithm based on the linearization of the cost function[17] is used: at a given point (X_0, Y_0) a linear approximation of Trace $(X^{-1}Y^{-1})$ is

$$\text{Trace}\,(X^{-1}Y^{-1}) \approx \text{constant} + \text{Trace}\left(X_0^{-1}Y^{-1} + X^{-1}Y_0^{-1}\right) \tag{9}$$

An iterative algorithm is then defined. From a feasible point (X_k, Y_k), find the point (X_{k+1}, Y_{k+1}) that solves the LMI problem:

$$\max_{X^{-1}, Y^{-1}} \text{Trace}\left(X_k^{-1}Y^{-1} + X^{-1}Y_k^{-1}\right) \tag{10}$$

subject to Eqs. (8). The convergence of this algorithm has been proven in Ref. 17.

The application of this reduction procedure on the LFT obtained earlier allows one to reduce the size of the interconnected matrix. Indeed the sizes of the parameter blocks (Fig. 3) have decreased to $n_M = 15$ and $n_z = 23$. Because this reduction algorithm can be applied on every LFT, it will be further used to reduce the LPV controller (Sec. IV.D).

IV. Controller Synthesis

A. Robust Stabilization for a Fixed Model

The H_∞/loop-shaping problem is considered as in Refs. 7 and 10. These studies have shown that this H_∞ problem is relevant because of two main reasons: it preserves a strong physical sense because of the open-loop shaping, as explained further, and it is known generally to provide good robustness qualities. The nominal model $G(s)$ is first shaped by introducing pre- and postcompensators $W_1(s)$ and $W_2(s)$ selected following the classical rules of automatic control. The nominal model is then replaced by the shaped one $G_a(s) = W_2(s)G(s)W_1(s)$.

The H_∞ problem to be solved is then: for $\gamma > 0$ as small as possible, find a stabilizing controller $K(s)$ such that

$$\left\| \begin{pmatrix} KS_aG_a & KS_a \\ S_aG_a & S_a \end{pmatrix} \right\|_\infty < \gamma \tag{11}$$

where $S_a(s) = [I + G_a(s)K(s)]^{-1}$ is the sensitivity function.

This problem corresponds to the minimization of the norm of the transfer from $(w_1 \;\; w_2)^T$ to $(e_1 \;\; e_2)^T$ (Fig. 4). The feedback controller is then $K_f(s) = W_1(s)K(s)W_2(s)$. The approach just described allows one to design an autopilot for a fixed flight point. An additional procedure has to be defined to consider various flight conditions.

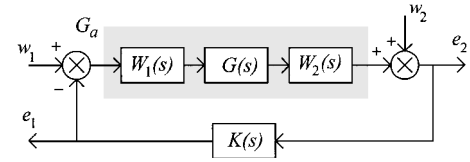

Fig. 4 Loop-shaping H_∞ problem.

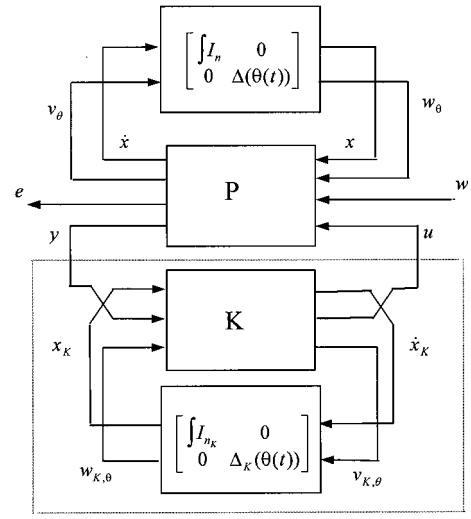

Fig. 5 General interconnection structure of the gain-scheduled closed-loop system.

B. Controller Synthesis of an LPV System with an L_2 Gain Constraint

The goal of this section is to outline the key results of the theory used to gain schedule the controller. More details can be found in Ref. 9.

The interconnection structure for the design of gain-scheduled controllers is depicted in Fig. 5, where

$$\boldsymbol{P} = \begin{bmatrix} A & B_\theta & B_1 & B_2 \\ C_\theta & D_{\theta\theta} & D_{\theta 1} & D_{\theta 2} \\ C_1 & D_{1\theta} & D_{11} & D_{12} \\ C_2 & D_{2\theta} & D_{21} & 0 \end{bmatrix}$$

denotes the state-space realization of the open-loop plant and

$$\boldsymbol{K} = \begin{bmatrix} A_K & B_{K1} & B_{K\theta} \\ C_{K1} & D_{K11} & D_{K1\theta} \\ C_{K\theta} & D_{K\theta 1} & D_{K\theta\theta} \end{bmatrix}$$

is the state-space realization of the controller. u, y, w, and e are respectively the control inputs, the measured outputs, the exogenous inputs, and the controlled outputs; $\theta(t) = [\theta_1(t), \ldots, \theta_L(t)]^T$ denotes the vector of the scheduling time-varying parameters; and $\Delta[\theta(t)]$ and $\Delta_K[\theta(t)]$ have the diagonal structures $\text{diag}[\theta_1(t)I_{r1}, \ldots, \theta_L(t)I_{rL}]$ with $|\theta_i(t)| \leq 1\ \forall t$ for $i = 1$ to L.

Let us define n (resp. n_K, m, p, r, and r_K) the size of x {resp. x_K, u, y, $\Delta[\theta(t)]$ and $\Delta_K[\theta(t)]$}. So, the plant is described by the upper LFT $F_u(\boldsymbol{P}, \text{diag}\{\int I_n, \Delta[\theta(t)]\})$ and the controller by the lower LFT

$$F_l\left(\begin{pmatrix} 0 & I_m & 0 \\ I_{n_K} & 0 & 0 \\ 0 & 0 & I_r \end{pmatrix} \boldsymbol{K} \begin{pmatrix} 0 & I_{n_K} & 0 \\ I_p & 0 & 0 \\ 0 & 0 & I_r \end{pmatrix}, \text{diag}\left\{\int I_{n_K}, \Delta_K[\theta(t)]\right\}\right)$$

The integration of the time-varying parameter vector $\theta(t)$ in the controller is expected to improve both the performance and the robustness of the closed-loop system, compared to an LTI controller.

The objective of the synthesis problem is to find $\boldsymbol{K}$ so that the closed-loop system of Fig. 5 is robustly stable, that is, stable for all admissible trajectories of $\theta(t)$ and has robust performance, that is,

the L_2 gain (which is the extension of the H_∞ norm) between e and w remains below γ for all trajectories of the parameters.[9]

The scaled bounded real lemma leads to sufficient conditions for the solvability of this problem. It is merely a refined version of the small gain theorem where the structure and the nature of $\mathrm{diag}\{\int I_n, \Delta[\theta(t)]\}$ are taken into account.

Let us define the following sets:

$$L_\theta = \{L = L^T > 0,\ L\Delta[\theta(t)] = \Delta[\theta(t)]L, \text{ for all admisible } \theta(t)\}$$

$$P_{\int} = \{P = P^T > 0\}$$

The matrices of L_θ commute with all matrices $\Delta[\theta(t)]$ while the matrices of P_f obviously commute with the integrators block $\int I_n$.

From the scaled bounded real lemma, the control problem just defined is solvable whenever there exist pairs of symmetric matrices (L, J) in L_θ and (R, S) in P_f so that

$$\begin{bmatrix} N_R & 0 \\ 0 & I \end{bmatrix}^T \begin{bmatrix} RA^T + AR & RC_\theta^T & RC_1^T & B_\theta J & B_1 \\ C_\theta R & -J & 0 & D_{\theta\theta} J & D_{\theta 1} \\ C_1 R & 0 & -\gamma I & D_{1\theta} J & D_{11} \\ JB_\theta^T & JD_{\theta\theta}^T & JD_{1\theta}^T & -J & 0 \\ B_1^T & D_{\theta 1}^T & D_{11}^T & 0 & -\gamma I \end{bmatrix} \begin{bmatrix} N_R & 0 \\ 0 & I \end{bmatrix} < 0$$

$$\begin{bmatrix} N_S & 0 \\ 0 & I \end{bmatrix}^T \begin{bmatrix} SA + A^T S & SB_\theta & SB_1 & C_\theta^T L & C_1^T \\ B_\theta^T S & -L & 0 & D_{\theta\theta}^T L & D_{1\theta}^T \\ B_1^T S & 0 & -\gamma I & D_{\theta 1}^T L & D_{11}^T \\ LC_\theta & LD_{\theta\theta} & LD_{\theta 1} & -L & 0 \\ C_1 & D_{1\theta} & D_{11} & 0 & -\gamma I \end{bmatrix} \begin{bmatrix} N_S & 0 \\ 0 & I \end{bmatrix} < 0$$

$$\begin{bmatrix} R & I \\ I & S \end{bmatrix} > 0, \qquad \begin{bmatrix} L & I \\ I & J \end{bmatrix} > 0 \tag{12}$$

where N_R, N_S are any bases of the null spaces of $\lfloor B_2^T \ \ D_{\theta 2}^T \ \ D_{12}^T \rfloor$ and $[C_2 \ \ D_{2\theta} \ \ D_{21}]$ (Ref. 9). From R, S, J, L, and γ a controller matrix $\boldsymbol{K}$ with $n_K = n$ and $\Delta_K[\theta(t)] = \Delta[\theta(t)]$ is obtained by solving the LMI:

$$\Psi + P_{X_{\mathrm{cl}}}^T \boldsymbol{K} Q + Q^T \boldsymbol{K}^T P_{X_{\mathrm{cl}}} < 0 \tag{13}$$

where

$$\Psi = \begin{bmatrix} A^T S + SA & A^T N & 0 & SB_\theta & SB_1 & 0 & C_\theta^T & C_1^T \\ N^T A & 0 & 0 & N^T B_\theta & N^T B_1 & 0 & 0 & 0 \\ 0 & 0 & -L_1 & -L_2 & 0 & 0 & 0 & 0 \\ B_\theta^T S & B_\theta^T N & -L_2^T & -L & 0 & 0 & D_{\theta\theta}^T & D_{1\theta}^T \\ B_1^T S & B_1^T N & 0 & 0 & -I & 0 & D_{\theta 1}^T & D_{11}^T \\ 0 & 0 & 0 & 0 & 0 & -J_1 & -J_2 & 0 \\ C_\theta & 0 & 0 & D_{\theta\theta} & D_{\theta 1} & -J_2^T & -J & 0 \\ C_1 & 0 & 0 & D_{1\theta} & D_{11} & 0 & 0 & -\gamma I \end{bmatrix}$$

$$Q = \begin{bmatrix} 0 & I & 0 & 0 & 0 & 0 & 0 & 0 \\ C_2 & 0 & 0 & D_{2\theta} & D_{21} & 0 & 0 & 0 \\ 0 & 0 & I & 0 & 0 & 0 & 0 & 0 \end{bmatrix}$$

$$P_{X_{\mathrm{cl}}} = \begin{bmatrix} N^T & E & 0 & 0 & 0 & 0 & 0 & 0 \\ B_2^T S & B_2^T N & 0 & 0 & 0 & 0 & D_{2\theta}^T & D_{12}^T \\ 0 & 0 & 0 & 0 & 0 & I & 0 & 0 \end{bmatrix} \tag{14}$$

with

$$\begin{bmatrix} S & N \\ N^T & E \end{bmatrix} = \begin{bmatrix} R & * \\ * & * \end{bmatrix}^{-1}, \qquad \begin{bmatrix} L_1 & L_2 \\ L_2^T & L \end{bmatrix} = \begin{bmatrix} J_1 & J_2 \\ J_2^T & J \end{bmatrix}^{-1}$$

In some cases, the LMI (13) is ill conditioned, and solutions are more easily found by using the following explicit formulas, which extend the results explained in Ref. 18 to the LPV models. Let

$$\varepsilon_{\max}^{-1} = \lambda_{\max}\left\lfloor P_{X_{\mathrm{cl}}}^{+}\left[\Psi - \Psi P_{X_{\mathrm{cl}}}^{\perp}\left(P_{X_{\mathrm{cl}}}^{\perp}\Psi P_{X_{\mathrm{cl}}}^{\perp T}\right)^{-1} P_{X_{\mathrm{cl}}}^{\perp T}\Psi\right] P_{X_{\mathrm{cl}}}^{+T}\right\rfloor$$

where $P_{X_{\mathrm{cl}}}^{+}$ denotes the pseudoinverse of $P_{X_{\mathrm{cl}}}$ and $P_{X_{\mathrm{cl}}}^{\perp}$ is a full rank matrix so that $P_{X_{\mathrm{cl}}} P_{X_{\mathrm{cl}}}^{\perp} = 0$, and

$$\Phi = (\varepsilon^{-1} P^T P - \Psi)^{-1} \qquad \text{where} \quad 0 < \varepsilon < \varepsilon_{\max}$$

Then the controller matrix is obtained as

$$\boldsymbol{K} = -\varepsilon^{-1} P_{X_{\mathrm{cl}}} \Phi Q^T (Q \Phi Q^T)^{-1} \tag{15}$$

In these solutions the interconnection block $\mathrm{diag}\{\int I_{n_K}, \Delta_K[\theta(t)]\}$ of the controller has the same structure and size as in the plant.

C. Design of the LPV-Shaped Plant

To incorporate the loop-shaping design objectives into the LPV synthesis, the transfer between w and e of Fig. 5 must correspond to the four-block criterion of Fig. 4. So the model used is the LPV-shaped plant obtained by the series connection of the LPV missile model and the compensators W_1 and W_2.

The missile model corresponds to the LPV model linearized for a stabilizing flight (see Sec. II); according to the H_∞/loop-shaping approach,[7] the compensators have to shape the open-loop frequency response. They are chosen with the following structure:

$$W_1(s) = [\omega_1/(\omega_1 + s)]I_3$$

$$W_2(s) = \mathrm{diag}(K_z + K_z'/s,\ K_q,\ K_y + K_y'/s,\ K_r,\ K_\varphi + K_\varphi'/s,\ K_p) \tag{16}$$

$W_1(s)$ is a roll-off filter whose cutoff frequency ω_1 is adjusted to attenuate the high-frequency sensor noise and to ensure the robustness against high-frequency modeling uncertainties, such as bending modes and neglected actuator or sensor dynamics. $W_2(s)$ includes first three scalar gains K_q, K_r, K_p (acting on q, r, p, respectively) that are used to adjust the bandwidth of the inner loop; it also includes proportional and integral control on a_z, a_y, φ in order to achieve zero steady errors. This structure is one of the three classical ones whose properties are discussed in Ref. 19: for each channel $W_2(s)$ exhibits three gains. According to Ref. 19, they have to be tuned to place the three dominant closed-loop poles or equivalently to obtain the required rise-time and stability margins, while maintaining a small overshoot in response to normal acceleration or roll angle step demands.

Six H_∞ syntheses for the six fixed flight points shown in Fig. 2 have been proceeded. For each of them, the parameters of $W_1(s)$ and $W_2(s)$ are tuned according to the rules just explained, while obtaining a value between 3 and 3.5 for the H_∞ norm (11). It has been found that the same filter $W_1(s)$ can be chosen for all syntheses, while $W_2(s)$ can be tuned with respect to the altitude z only. The nine gains of $W_2(s)$ are then interpolated by a least-squares procedure, where each of them is expressed as a third-order polynomial on z.

The LPV model of the shaped plant is then obtained by the series connection of the LPV missile model and the LPV compensators. The multidimensional reduction procedure (Sec. III) allows us to formulate the shaped plant by an LFT as shown on Fig. 5 with $\int I_n = \int I_{21}$ and $\Delta[\theta(t)] = \mathrm{diag}(MI_{15}, zI_{58})$.

D. Controller Synthesis and Reduction

The solutions of the LMI (12) and (13) lead to a controller $\boldsymbol{K}$ as shown in Fig. 5. The interconnected matrix $\mathrm{diag}\{\int I_{n_K}, \Delta_K[\theta(t)]\}$ has the same structure and the same size as for the shaped plant.

Once again, the multidimensional reduction algorithm explained in Sec. III.B is then executed. The reduction is very efficient because it allows one to replace the 73×73 matrix $\Delta_K[\theta(t)]$ with a much simpler block zI_3. It means that the LPV controller $\boldsymbol{K}$ does not depend at all on the Mach number. This result is somewhat surprising because the variations of M are large, with significant effect on the dynamics; however, one can see in Fig. 2 that for each value of z the

Table 1 Gain, phase, and delay margins

Channel	Equivalent-loop minimum values	Equivalent-loop mean values	Outer-loop minimum values	Outer-loop mean values
Pitch channel	10.1 dB	13.6 dB	13.2 dB	22.3 dB
	40.5 deg	52.2 deg	41.4 deg	48.3 deg
	0.16τ	0.33τ	0.33τ	0.82τ
Yaw and roll channels	7.9 dB	10.9 dB	9.0 dB	12.8 dB
	30.8 deg	37.7deg	29.7 deg	38.1 deg
	0.11τ	0.21τ	0.28τ	0.44τ

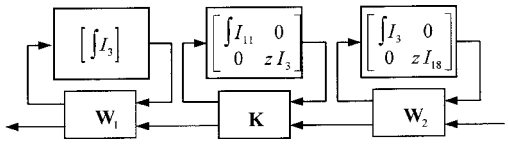

Fig. 6 Final gain-scheduled controller.

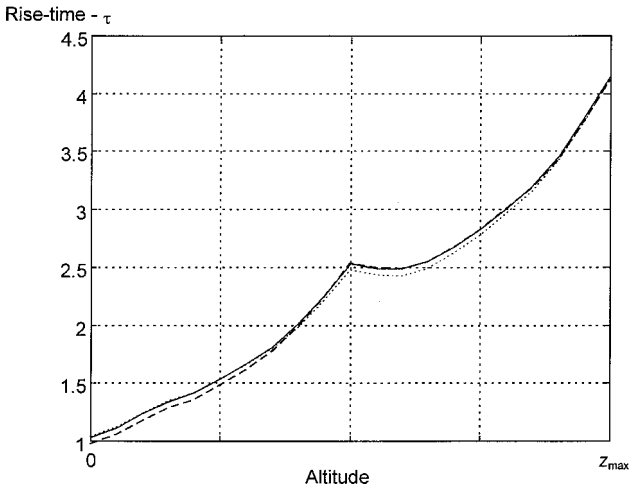

Fig. 7 Rise times over three trajectories of the pitch channel: ——, Mach nominal; - - - -, Mach − 0.1; · · · · ·, Mach +0.1.

possible values of M are within a narrow interval, so that scheduling the controller with respect to z takes implicitly into account the variations of M.

Besides, a modal reduction procedure[20] is applied to reduce the number of integrators of the controller: the original matrix $\int I_{21}$ is then replaced by $\int I_{11}$. Keeping in mind that the postcompensator $W_2(s)$ has to be scheduled, the final autopilot is obtained as shown in Fig. 6 in which the LPV compensators are described by their state-space realization written as an LFT.

V. Linear Analysis of the Gain-Scheduled Autopilot

In this section the behavior of the scheduled autopilot is analyzed for 41 linear models over each of three trajectories: the nominal one, the −0.1 Mach-shifted one, and the +0.1 Mach-shifted one. These three possible evolutions allow one to cover the entire flight envelope.

A. Time-Domain Performance

Linear simulations over the flight envelope were carried out. The rise time vs altitude is displayed in Fig. 7 for the pitch axis and in Fig. 8 for the roll axis. The rise times evolve regularly according to the altitude and are almost independent of the Mach number. The maximal values of the actuator input derivatives are also checked and are satisfying in all cases.

B. Stability Analysis

Gain, phase, and delay margins are evaluated at points 1 (equivalent loop) and 2 (outer loop) (Fig. 1). As stabilizing flight models are considered, there is an exact decoupling between the pitch channel and the roll and yaw channels. The margins of the pitch channel are classically evaluated from the open-loop frequency response.

To evaluate the multivariable gain margin of the yaw and roll channels, diagonal gain uncertainties are added to the plant, and

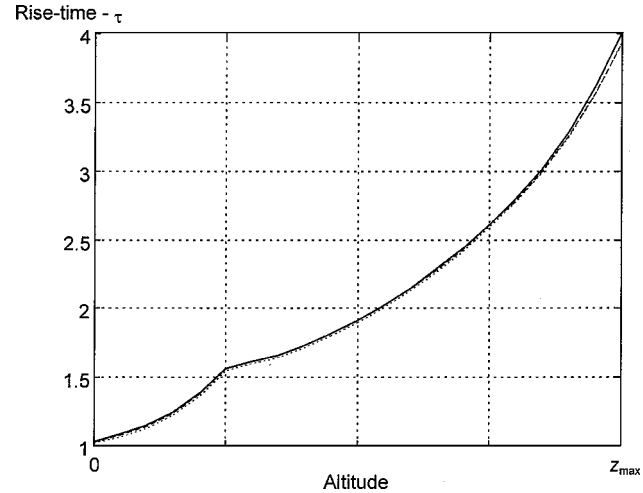

Fig. 8 Rise times over three trajectories of the roll channel: ——, Mach nominal; - - - -, Mach − 0.1; · · · · ·, Mach +0.1.

the structured singular value (ssv) is computed. In the same way multivariable phase and delay margins are obtained by considering phase and delay uncertainties. More information is given in Ref. 10 about such a computation of multivariable margins.

Table 1 shows the minimum and the mean values of gain, phase, and delay margins obtained over the full envelope for the equivalent and outer loops. The margins obtained are satisfying for all of the points.

C. Robust Stability Analysis

To check the robust stability, 41 uncertain linear models are considered over each of the three trajectories already defined. The uncertainties come from the ill-known 15 aerodynamic coefficients. The specified dispersions are between 10 and 45%. The resulting uncertain models are written as LFT, as explained in Ref. 10, in which the interconnected matrix Δ is a 15×15 diagonal matrix.

Then, the robustness of the design in the face of such parametric uncertainties has been analyzed using μ analysis.[11] Because the coupling terms between the pitch channel and the others channels are negligible, two separate μ analyses are conducted. As shown in Figs. 9 and 10, the maximum values of μ are less than one for both kinds of models, and so stability is guaranteed for uncertainties higher than the specified dispersions.

D. Performance Analysis

First, the H_∞ norms (11) of all of the linearized models already considered are computed and displayed in Figs. 11 and 12. The values are very homogeneous all over the envelope. It had been also noticed that the values are only 10 to 20% higher than those obtained by performing separate H_∞ optimizations for fixed values of M and z.

Second, the performance analysis is performed by determining the L_2 gain of the LPV system. With the L_2 gain being computed using an LMI, the parameters of the system have to evolve in a convex set. The flight envelope of Fig. 2 is therefore divided into two convex domains, namely a parallelogram covering the altitudes below $z_{\max}/2$ and a rectangle covering altitudes over $z_{\max}/2$. The following values are obtained: 1) pitch channel—6.78 at low altitude, 6.09 at high altitude; and 2) yaw/roll channel—4.68 at low altitude, 6.10 at high altitude.

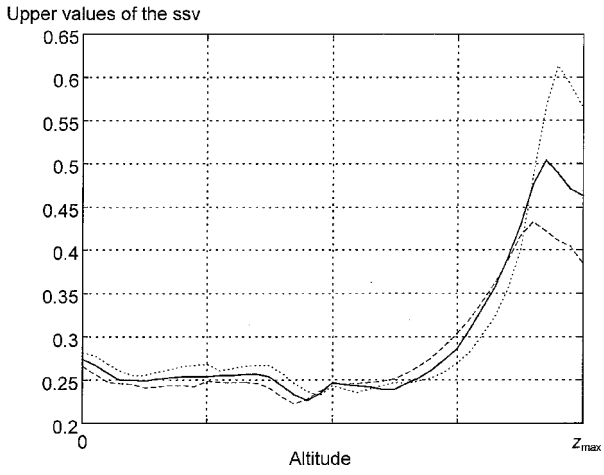

Fig. 9 Upper values of the ssv (pitch channel): ——, Mach nominal; - - - -, Mach − 0.1; · · · · ·, Mach +0.1.

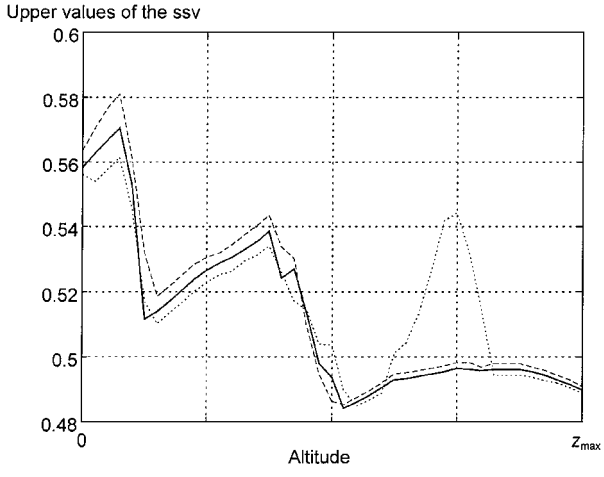

Fig. 10 Upper values of the ssv (yaw and roll channels): ——, Mach nominal; - - - -, Mach − 0.1; · · · · ·, Mach +0.1.

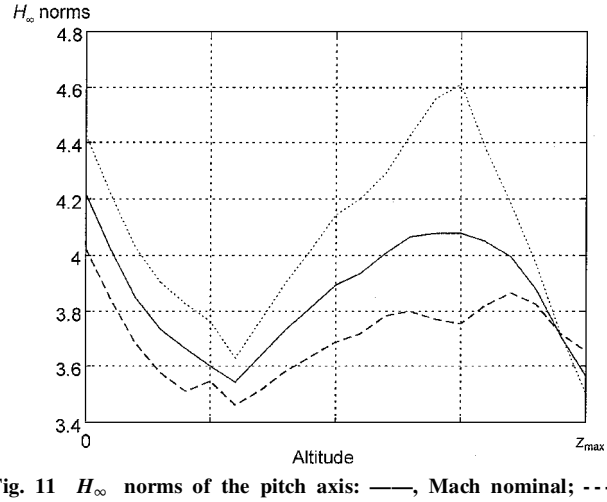

Fig. 11 H_∞ norms of the pitch axis: ——, Mach nominal; - - - -, Mach − 0.1; · · · · ·, Mach +0.1.

These results are very satisfactory because they are close to the H_∞ norms already obtained for LTI systems. It means that the LPV controller can handle the parameter variations in order to avoid disturbing the controlled plant a lot.

VI. Nonlinear Simulations

In this section the LPV controller is tested with a nonlinear model of the plant, where the aerodynamic forces and moments depend on M, z, α, and β. Two kinds of simulations around two distant points of the flight envelope have been proceeded: 1) step responses on pitch (Fig. 13) and roll (Fig. 14) channels with $z = 0$ and $M = M_{\min}$ as initial conditions; 2) step responses on pitch (Fig. 15) and roll (Fig. 16) channels with $z = z_{\max}$ and $M = M_{\max}$ as initial conditions. In both cases the nonlinear simulation proceeds 20 different step responses with perturbations on the aerodynamic coefficients generated by the Monte Carlo method. The amplitudes of the step demand correspond to the maximum values acceptable for this missile. Of course those values differ a lot for the two flight points selected.

These simulations allow us to confirm the good behavior already noticed in the linear case and reflect the actual performance of the missile in a better way. The responses are very homogeneous: they underline that the design has very good robustness properties. In all cases the overshoot is small, and the rise-time requirement is satisfied. It has also been verified that the sideslip angle, and the rates and accelerations of the executed fin deflections remain below their maximal allowable values. The low-altitude point also emphasizes the robustness of the LPV controller in regard to significant

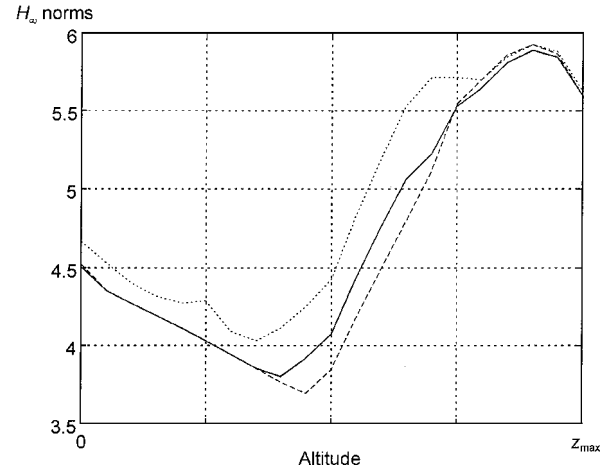

Fig. 12 H_∞ norms of the yaw and roll axis: ——, Mach nominal; - - - -, Mach − 0.1; · · · · ·, Mach +0.1.

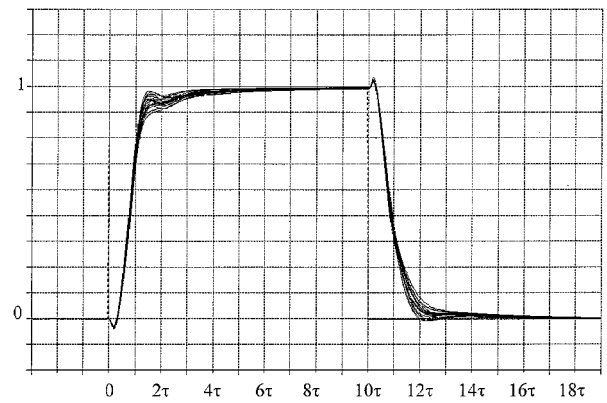

Fig. 13 Step responses of perturbed models (pitch channel) at low altitude.

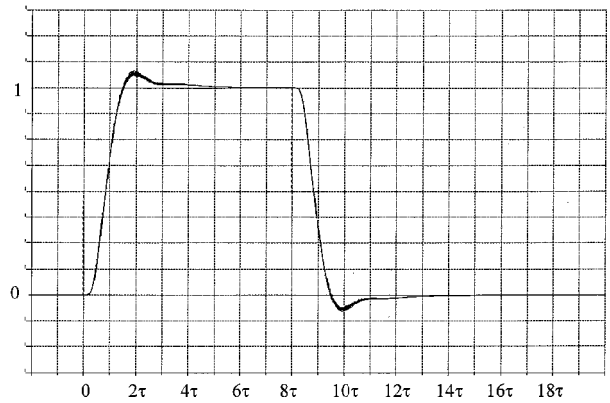

Fig. 14 Step responses of perturbed models (roll channel) at low altitude.

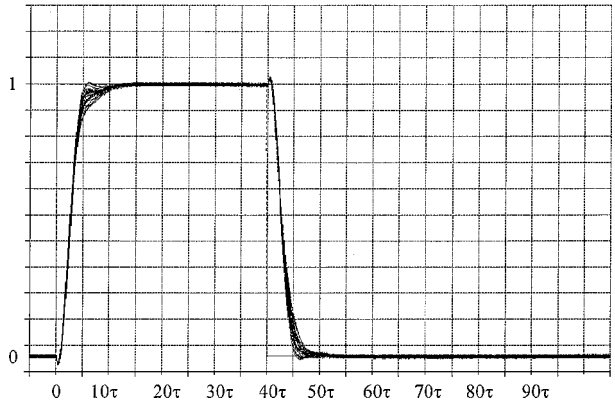

Fig. 15 Step responses of perturbed models (pitch channel) at high altitude.

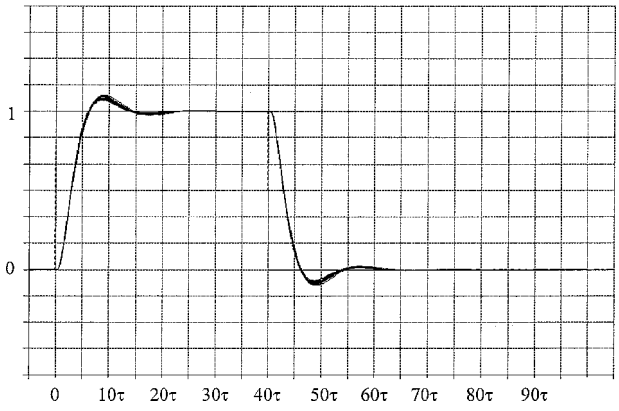

Fig. 16 Step responses of perturbed models (roll channel) at high altitude.

variations of the angle of attack. The high-altitude point brings into light the performance requirements. From a physical point of view, these two tests are a good indicator of the performance obtained on the whole flight domain.

This approach has been compared to the interpolation of H_∞ controllers designed for fixed flight conditions by considering the pitch channel.[21] Time and frequency domain performances are almost similar: it is not surprising to notice that the interpolated H_∞ controller performs better if the flight conditions are fixed, whereas the LPV controller yields better performance in case of fast variations of the scheduling parameters. From a practical point of view, the synthesis of the interpolated H_∞ controller reveals that to be more tedious in tuning the design parameters.

VII. Conclusions

In this paper a framework is applied to gain-schedule controllers in operational cases. It associates the H_∞/loop-shaping design, the LPV system theory, and a multidimensional reduction algorithm. It requires an LPV system model and LPV open-loop compensators that are obtained using interpolation over a few number of flight points. They allow the designer to adjust the specifications of the open-loop according to the value of the parameters.

The LPV-shaped plant is then formulated by an LFT. The use of the parametric multidimensional reduction procedure based on the generalized grammians reduces the size of this LFT.

The gain-scheduling approach allows us to obtain the LPV controller in just one step by solving LMIs. Then the number of state variables can be reduced by using classical algorithms. Once again, the multidimensional reduction procedure is carried out in order to reduce significantly the dependence of the controller on the scheduling parameters.

This technique has been successfully applied to a six-DOF missile autopilot design. Because of the efficiency of the reduction procedure, the resulting controller depends only on the altitude and has 11 state variables. It satisfies the specifications over a wide operating envelope. Robustness analyses and nonlinear six-DOF simulations have shown that the controller performs well in case of perturbed models.

This application has put in light three main points. First, the evolution of the specifications over the whole operating envelope is taken into account by using LPV compensators. Second, the LPV H_∞ controller is easily obtained by solving LMIs. Third, the resulting controller is not a complex one and could be easily implemented. These points show how practical and interesting this framework is in operational cases.

References

[1]Williams, D. E., Friedland, B., and Madiwale, A. N., "The Application of Scheduled H_∞ Controllers to a VSTOL Aircraft," *Journal of Guidance, Control, and Dynamics*, Vol. 10, No. 4, 1987, pp. 378–386.

[2]Reichert, R., "Dynamic Scheduling of Modern-Robust-Control Autopilot Design for Missiles," *IEEE Control Systems*, Vol. 12, No. 5, 1992, pp. 35–42.

[3]Nichols, R. A., Reichert, R. T., and Rugh, W. J., "Gain-Scheduling for H_∞ Controllers: A Flight Control Example," *IEEE Transactions on Control Systems Technology*, Vol. 1, No. 2, 1993, pp. 69–78.

[4]Carter, L. H., and Shamma J. S., "Gain-Scheduled Bank to Turn Autopilot Design Using Linear Parameter Varying Transformations," *Journal of Guidance, Control, and Dynamics*, Vol. 19, No. 5, 1996, pp. 1056–1063.

[5]Biannic, J. M., Apkarian, P., and Gahinet, P., "Self-Scheduled H_∞ Control of Missiles via Linear Matrix Inequalities," *Journal of Guidance, Control, and Dynamics*, Vol. 18, No. 3, 1995, pp. 532–538.

[6]Fialho, I., Balas, G. J., Packard, A. K., Renfrow, J., and Mullaney, C., "Gain-Scheduled Lateral Control of the F-14 Aircraft During Powered Approach Landing," *Journal of Guidance, Control, and Dynamics*, Vol. 23, No. 3, 2000, pp. 450–458.

[7]McFarlane, D., and Glover, K., "A Loop-Shaping Design Procedure Using H_∞-Synthesis," *IEEE Transactions on Automatic Control*, Vol. 37, No. 6, 1992, pp. 759–769.

[8]Beck, C., Doyle, J., and Glover, K., "Model Reduction of Multi-Dimensional and Uncertain Systems," *IEEE Transactions on Automatic Control*, Vol. 41, No. 10, 1996, pp. 1466–1477.

[9]Apkarian, P., and Gahinet, P., "A Convex Characterization of Gain-Scheduled H_∞ Controllers," *IEEE Transactions on Automatic Control*, Vol. 40, No. 5, 1995, pp. 853–864.

[10]Friang, J. P., Duc, G., and Bonnet, J. P., "Robust Autopilot for a Flexible Missile: Loop-Shaping H_∞ Design and Real ν Analysis," *International Journal of Robust and Nonlinear Control: Special Issue on Robust Control Applications*, Vol. 8, No. 2, 1998, pp. 129–153.

[11]Zhou, K., Doyle, J., and Glover, K., *Robust and Optimal Control*, Prentice–Hall, Upper Saddle River, NJ, 1996, pp. 247–300.

[12]Lambrechts, P., Terlouw, J., Bennani, S., and Steinbuch, M., "Parametric Uncertainty Modelling Using LFTs," *Proceedings of the American Control Conference*, IEEE Publications, Piscataway, NJ, 1993, pp. 267–272.

[13]Wang, W., Doyle, J., Beck, C., and Glover, K., "Model Reduction of LFT Systems," *30th IEEE Conference on Decision and Control*, IEEE Publications, Piscataway, NJ, 1991, pp. 1233–1238.

[14]Beck, C., "Minimality for Uncertain Systems and IQCs," *33rd IEEE Conference on Decision and Control*, IEEE Publications, Piscataway, NJ, 1994, pp. 3068–3073.

[15]El Ghaoui, L., and Gahinet, P., "Rank Minimization Under LMI Constraints: A Framework for Output Feedback Problems," *Proceedings of the 2nd European Control Conference ECC'93*, edited by J. W. Nieuwenhuis, C. Praagman, and H. L. Trentelman, Vol. 3, 1993, pp. 1176–1179.

[16]Hiret, A., Valentin-Charbonnel, C., Duc, G., and Bonnet, J. P., "Different Multidimensional Reduction Algorithms for the LFT Model of a Missile," *2nd IMACS International Multi-Conference CESA'98*, 1998.

[17]El Ghaoui, L., Oustry, F., and AitRami, M., "A Cone Complementarity Linearization Algorithm for Static Output-Feedback and Related Problems," *IEEE Transactions on Automatic Control*, Vol. 42, No. 8, 1997, pp. 1171–1176.

[18]Iwasaki, T., and Skelton, R. E., "All Controllers for the General H_∞ Control Problem: LMI Existence Conditions and State Space Formulas," *Automatica*, Vol. 30, No. 8, 1994, pp. 1307–1317.

[19]Horton, M. P., "Autopilots for Tactical Missiles: An Overview," *Journal of Systems and Control Engineering*, Vol. 209, No. 12, 1995, pp. 127–139.

[20]Siret, J. M., Michailesco, G., and Bertrand, P., "On the Use of Aggregation Techniques," *Handbook of Large Scale Systems Engineering Applications*, edited by M. Singh and A. Titli, North-Holland, Amsterdam, 1979, pp. 20–37.

[21]Hiret, A., Duc, G., and Bonnet, J. P., "The Application of Gain-Scheduling H_∞ Controllers for a Missile Autopilot," *Proceedings of the 14th IFAC Symposium on Automatic Control in Aerospace*, Pergamon, Oxford, England, U.K., 1998, pp. 65–70.